Chemisorption of Molecular Hydrogen on Carbon Nanotubes: A Route to Effective Hydrogen Storage?

ARTICLE *in* THE JOURNAL OF PHYSICAL CHEMISTRY C · JULY 2008

Impact Factor: 4.77 · DOI: 10.1021/jp802104n

2 AUTHORS:

Ante Bilic
The Commonwealth Scientific and Industri…
68 PUBLICATIONS **1,047** CITATIONS
SEE PROFILE

Julian David Gale
Curtin University
270 PUBLICATIONS **14,942** CITATIONS
SEE PROFILE

Chemisorption of Molecular Hydrogen on Carbon Nanotubes: A Route to Effective Hydrogen Storage?

Ante Bilić*,† and Julian D. Gale‡

Materials Theory and Simulations Laboratory, Institute of High Performance Computing, 1 Science Park Road, #01-01 The Capricorn, Singapore Science Park II, Singapore 117528, and Nanochemistry Research Institute, Department of Applied Chemistry, Curtin University of Technology, P.O. Box U1987, Perth 6845, Western Australia

Received: March 10, 2008; Revised Manuscript Received: May 20, 2008

The energetics of the chemisorption of molecular hydrogen on small-diameter armchair carbon nanotubes has been investigated using first-principles density functional theory (DFT). The adsorption of hydrogen was examined at a range of coverages, from low to full monolayer coverage. Several pathways for hydrogenation were investigated, and those that could lead to energetically favorable, stable structures of fully saturated nanotubes were identified. For these routes, the calculations indicate that the addition of hydrogen, apart from at the very onset, is exothermic and also becomes increasingly more favorable with increasing degree of coverage. Carbon nanotubes of sufficiently small diameter are shown to have the capacity to store a full monolayer of hydrogen effectively via chemisorption. In addition, kinetic barriers for the dissociative chemisorption of H_2 and thermal equilibration of the system were considered. These were found to be quite large for admolecules on an otherwise-clean nanotube, but to drop substantially in the vicinity of preadsorbed hydrogen; that is, the adsorbed hydrogen acts as an autocatalyst for further hydrogenation. On the basis of these findings, the chemical reaction of hydrogen with carbon nanotubes is expected to become increasingly exothermic and also to proceed more rapidly at higher coverages.

I. Introduction

Hydrogen is frequently touted as the "fuel of the future" because of its huge potential as a clean energy source, although the large-scale adoption of this technology has yet to be realized. One of the remaining barriers to the utilization of hydrogen energy is an efficient and inexpensive means of hydrogen storage. To this end, carbonaceous materials, among others, have been considered because of their stability; low weight; and porosity, resulting in large specific surface areas. However, their uptake of hydrogen is generally well below 6.5 wt %,[1] which is the target set by the U.S. Department of Energy (U.S. DOE) for on-board storage in hydrogen-powered vehicles.

Shortly after the discovery of carbon nanotubes (CNTs), their storage capacity was investigated in the pioneering work of Dillon et al.[2] Measuring the sorption of hydrogen in a soot containing only a small fraction of CNTs, Dillon et al. observed a total uptake of 0.01 wt % and attributed it solely to bundles of single-walled nanotubes (SWNTs). In this manner, they obtained an unusually high uptake of hydrogen gas of 5−10 wt % by SWNTs. They attributed this phenomenon to the enhanced physisorption of hydrogen inside individual tubes (endohedral adsorption) and in the interstitial regions of bundles (exohedral adsorption), which results in a binding energy of 19.6 kJ mol^{-1} or, conversely, in an adsorption energy of −0.2 eV per molecule, using the convention and units of the present study. The findings of Dillon et al. have served as the motivation for considerable research effort in this field in recent years. However, a number of related studies that followed could not reproduce those results, and usually, a lower uptake was reported,[3] thus adding controversy to the subject. The controversy arises in part because of the poor characterization of the carbon substrate, which frequently comprises both single- and multiwalled nanotubes of varying diameters and chiralities, with both capped and open ends.

Theoretical investigations of H_2 physisorption in nanotubes typically predict a somewhat stronger interaction of hydrogen with an SWNT than with graphite, but this effect of surface curvature is insufficient to account for a substantial increase in uptake.[4–6] A further enhancement to the interaction is found if dynamic deformations[7] and defects[8–10] in SWNTs are taken into account, but even such effects cannot explain the anomalously high values of hydrogen uptake in CNTs based on pure physisorption.[8]

Hydrogen storage in CNTs by chemical reaction, on the other hand, has largely been discounted as irreversible and thus technologically less relevant. Whereas the release of chemically stored hydrogen is not as facile as that of physisorbed hydrogen, given the controversy of the latter, the topic deserves careful consideration for several reasons. First, the reproducible experiments of Liu et al.[3] demonstrate that, of the 4.2 wt % hydrogen that is adsorbed at moderate pressures and room temperature, 78.3% (3.3 wt %) is physisorbed, whereas the extraction of residual stored hydrogen (0.9 wt %) requires heating to 473 K and above. This suggests that some form of chemical adsorption occurs at room temperature. Second, it has been shown that CNTs are capable of storing a modest amount of hydrogen electrochemically.[11,12] Third, under a high applied pressure of hydrogen, a first-order phase transformation in CNTs has been reported, which is reminiscent of hydride phases in metal−hydrogen systems.[13] It was demonstrated recently that the high-pressure hydrogenation of SWNTs results in H covalently bound to C at ∼4.7 wt % and interstitial H_2 at ∼0.5 wt %.[14] In addition, novel procedures using hydrogen plasma[15–18] and polyamine reagents[19] have been harnessed to achieve a sizable degree of chemical hydrogenation in SWNTs. Finally, a highly nonequi-

† Institute of High Performance Computing.
‡ Curtin University of Technology.

10.1021/jp802104n CCC: $40.75
Published on Web 07/18/2008

librium method of CNT hydrogenation by the implantation of molecular and atomic hydrogen beams has been proposed.[9,20] Recent experimental studies[21,22] have demonstrated that a high degree of hydrogenation of SWNTs, 65 ± 15% (5.1 ± 1.2 wt %), can be achieved with atomic H beams and that, just as importantly, the process is reversible.

Computational studies[9,20] have been performed using molecular dynamics based on an empirical many-body reactive force field. However, most computational investigations of hydrogen chemisorption in CNTs utilize more accurate density functional theory (DFT)[6,7,23–27] and also DFT-based tight-binding models.[28–31]

This work presents a computational study of hydrogen chemisorption for a small-diameter CNT, where the effects of curvature are accentuated. The principal interest of this study was to investigate the tendency of CNTs to hydrogenate and assess their capacity for hydrogen storage. Whereas most previous studies focused on either the interaction of a single H_2 admolecule with a clean CNT or the stability of heavily hydrogenated nanotubes, the current work addresses the energetics of chemisorption over a range of coverages, starting with a single admolecule and proceeding to a full monolayer (ML) of hydrogen. The results suggest that hydrogen chemisorption, apart from the very onset, is energetically favorable and that a small-diameter SWNT can adsorb a full monolayer of atomic hydrogen exothermically; thus, an uptake of hydrogen in excess of the 6.5 wt % target is predicted to be possible. The results for the kinetics of the chemisorption indicate rather large potential energy barriers to adsorbate dissociation and attachment on the CNT for isolated H_2 molecules. However, in the presence of other admolecules, the barriers are significantly reduced. The hydrogenation of the CNT is thus predicted to become more favorable and also to advance at an increasing rate with increasing coverage.

This article is organized as follows: In section II, the methods and models of the nanotubes are described. In Sec. III results for the energetics of chemisorption are presented and for the most favorable pathways of initial hydrogenation, kinetic barriers for dissociative adsorption are computed. The relevance of the current findings for the realistic use of nanotubes for hydrogen storage is discussed in the context of results from related studies and summary is given in Sec. IV.

II. Computational Methodology

The computations were performed using the SIESTA program.[32,33] In the SIESTA methodology for performing density functional theory calculations, a linear combination of atomic orbitals (LCAO) is used to to expand the Kohn−Sham wave functions. Core electrons and nuclei are replaced by norm-conserving pseudopotentials in fully separable form.[34] The scheme of Troullier and Martins[35] was employed to generate pseudopotentials for both hydrogen and carbon, with relativistic corrections included for the latter. For the exchange and correlation potential, the PBE functional,[36] a form of generalized gradient approximation (GGA), was used both for pseudopotential generation and for the actual calculations. The one-electron Kohn−Sham eigenstates were expanded in a basis of strictly localized[37] numerical pseudo-atomic orbitals.[38] Basis functions were obtained by finding the eigenfunctions of the isolated atoms confined within a sphere. The range of the atomic orbitals was chosen so as to obtain an energy increase of 2.5 mRy arising as a result of the spherical confinement. A split valence scheme was employed to generate a triple-ζ basis set for the 1s states of H and the 2s and 2p states of C, with a single-ζ shell of polarization functions for hydrogen and carbon. SIESTA uses an auxiliary real-space mesh to evaluate terms based on charge density, and an equivalent plane-wave cutoff of 150 Ry was used to determine the mesh spacing.

Several armchair CNTs were considered as the model of the carbon substrate and eventually a (6,6) SWNT was selected as most appropriate because of its relatively small size and its feasibility for synthesis. Both finite and infinite models of the nanotube were employed. In the finite model, the tube was taken to consist of 10 atomic layers of carbon, both ends of which were terminated with hydrogen atoms, placed in a cubic periodic supercell with sides of 21 Å. The infinite model of the tube was represented by an eight-atomic-layer repeat, corresponding to a supercell containing four basic cells, placed in an orthogonal periodic supercell with lateral sides of 18 Å. By optimizing the periodic repeat direction of the cell only, a length of 9.980 Å for the supercell was obtained, resulting in C—C bond lengths of 1.444 Å. The application of periodic boundary conditions in all three Cartesian directions yielded an infinite array of periodically repeated SWNTs separated by regions of vacuum to prevent interactions with atoms in adjacent cells.

Because of the metallic character of armchair nanotubes, the total energy convergence with respect to Brillouin-zone sampling is quite important. With a grid of 10 k points in the direction parallel to the tube axis, the total energy was found to converge to better than 10 meV. Calculations involving either the finite model of the SWNT or a gas-phase hydrogen molecule were carried out at the Γ point only, and for the latter, a cell of the same size as that for the (6,6) SWNT was used. The results for the energy minima employed spin-restricted (i.e., closed-shell) computations. However, the searches for transition states that define kinetic barriers to chemisorption were conducted with spin-polarized (i.e., unrestricted open-shell) calculations in order to reproduce the correct dissociation limit of the H_2 molecule. Only the Γ point was utilized for the latter so as to reduce the computational cost. All atomic geometries were relaxed via the action of a conjugate gradient optimization procedure until the forces acting on the atoms were below 0.01 eV Å^{-1}.

III. Results and Discussion

The energetics of the chemical reaction is expressed through the average adsorption energy per hydrogen molecule,[45] which is defined as

$$E_a(n) = (E^{tot}_{nH_2+NT} - E^{tot}_{NT} - nE^{tot}_{H_2})/n \quad (1)$$

Here, E^{tot}_{NT}, $E^{tot}_{H_2}$, and $E^{tot}_{nH_2}$+NT are the total energies of the isolated CNT, gas-phase H_2, and the CNT hydrogenated by n molecules of hydrogen per supercell, respectively. The binding strength is deliberately taken relative to H_2, which is the ground-state of hydrogen, rather than to atomic hydrogen. According to this definition, a negative adsorption energy corresponds to a favorable, exothermic structure of the complex. The strain energy, that is, the energy of the distortion of C—C bonds due to H adsorption, is defined as

$$E_s = E^{tot}_{NT,dist} - E^{tot}_{NT} \quad (2)$$

where $E^{tot}_{NT,dist}$ is the total energy of a clean CNT calculated in the distorted geometry obtained following hydrogenation but with the hydrogens removed.

To identify an appropriate choice of CNT for subsequent computations, the adsorption energy for a single H_2 molecule as a function of tube size was first evaluated for the two most favorable adsorption geometries, termed 1−2d and 1−2v, as illustrated in Figure 1. The results of these calculations are

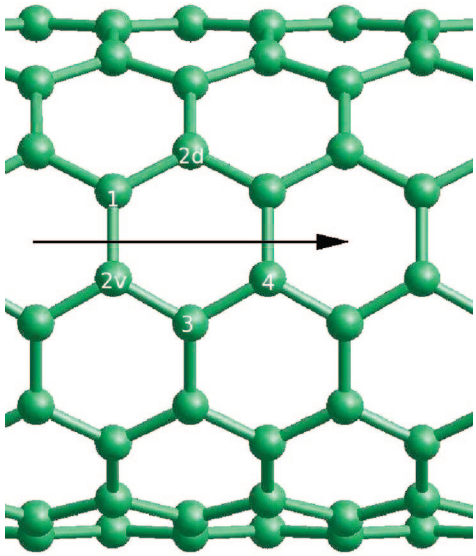

Figure 1. Sites 1, 2v, 2d, 3, and 4 for H_2 dissociative attachment. The periodic repeat direction of the tube runs from left to right, as indicated by the arrow.

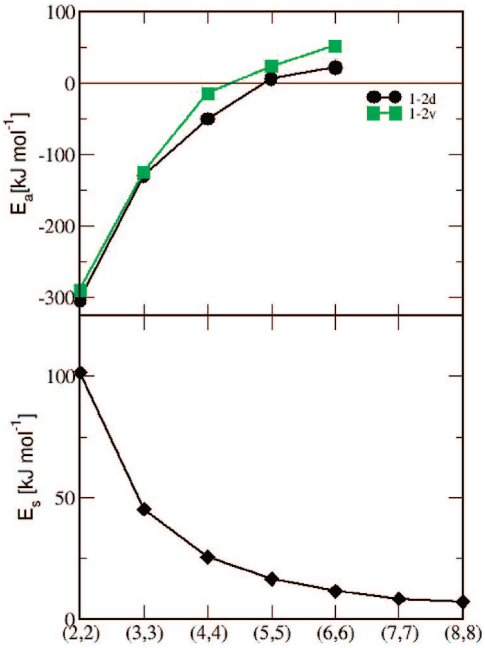

Figure 2. (Top) Adsorption energy for H_2 dissociatively adsorbed on an armchair SWNT as a function of tube size. The adsorption geometries 1−2d and 1−2v (cf. Figure 1) were considered. (Bottom) Strain energy relative to a graphene sheet for an SWNT as a function of tube size.

shown in the upper panel of Figure 2. It is evident that the adsorption becomes endothermic only for SWNTs with diameters equal to, or larger than, that of a (5,5) armchair tube. (In general, hydrogenated zigzag and armchair CNTs with similar radii exhibit quite comparable binding strengths.[25]) The lower panel in Figure 2 shows the strain energy as a function of tube size. It is clear that, for SWNTs with diameters greater than that of a (5,5) nanotube, the energy decreases rather slowly to the asymptotic limit of that of a graphene sheet. Therefore, a (6,6) SWNT was chosen as a realistic representation of a feasible carbon substrate to model the chemical reaction with hydrogen. Coincidentally, a very similar geometry for the CNT (and a similar SIESTA methodology) was employed in a very recent study.[19] However, this previous work utilized the local density approximation (LDA), as opposed to the GGA approach as used in the present work.

TABLE 1: Adsorption Energies, E_a (eV), for the Dissociative 1−2v, 1−2d, 1−3, and 1−4 Exoadditions of H_2 on a (6,6) SWNT

conformation	E_a (eV)
1−2v	0.535
1−2d	0.220
1−3	1.676
1−4	0.475

The hydrogenation was first studied in the low-coverage limit, by considering the dissociative chemisorption of a single molecule on the outer face of a (6,6) SWNT. This was first performed on the infinite model of the tube. Four possible modes of hydrogen addition were considered, labeled 1−2v, 1−2d, 1−3, and 1−4, which indicate that, if one of the H atoms is bound to a C atom labeled 1, then the other H atoms can bond to one of the following sites: the initial H atom's first neighbor along the C—C bond that is vertical (orthogonal) to the tube axis (label 2v), its first neighbor along a C—C bond that is "diagonal" to the axis (2d), a C atom that is at point 3 in the same benzene-like ring, or a C atom that is located on the opposite side (i.e., point 4) in the same hexagon. A similar terminology was recently used by others.[39,40] The first two cases fall under the "ortho" category, whereas 1−3 would then be named "meta" and 1−4 would be named "para", in analogy with substituitional benzene isomers.[19] These sites are illustrated in Figure 1. No endohydrogenation (hydrogen on the inner face) was considered in this limit because the geometry constraints make the formation of sp^3 bonds on two adjacent C atoms highly strained and unfavorable.[24]

The adsorption energies for the four exosites are given in Table 1. Two interesting observations can be made. First, the energies are positive, predicting that the dissociative chemisorption is not favorable. Second, the calculations suggest that the molecule preferentially adsorbs in the 1−2d conformation. It is also worth noting that the 1−3 hydrogen exoaddition is the least favorable. It is not clear why the 1−2d exoaddition appears more favorable than 1−2v, given that the C—C bonds that are perpendicular to the tube axis are more strained than diagonal bonds. In fact, DFT results in the literature favor the 1−2v exoadditon of H_2.[6,23,26,27] However, those results were evaluated for moderate and high hydrogen coverages, specifically, one and two H_2 molecules per two unit cells, whereas the present results are pertinent to one admolecule per four unit cells. On the other hand, the recent results of Miller et al.[19] are in agreement with ours.

An endothermic H_2/SWNT chemisorption reaction in the low-coverage limit was reported in previous DFT studies,[6,23–25] and in that respect, the present results are in agreement with these earlier works. However, DFT-based calculations show that heavily hydrogenated CNTs are stable.[25,26,28–31] Obviously, many isomers could exist for a hydrogenated SWNT, and we do not make an attempt to investigate all possibilities. To investigate the trends of hydrogenation, we defined a chemical potential that indicates how favorable it is to adsorb an additional H_2 molecule on an already partially protonated CNT

$$\mu = E^{\mathrm{tot}}_{n\mathrm{H}_2+\mathrm{NT}} - E^{\mathrm{tot}}_{(n-1)\mathrm{H}_2+\mathrm{NT}} - E^{\mathrm{tot}}_{\mathrm{H}_2} = nE_a(n) - (n-1)E_a(n-1) \quad (3)$$

It corresponds to the rate of change of the binding strength with hydrogen coverage. As with the adsorption energy, a negative

TABLE 2: Adsorption energy, E_a and chemical potential μ (eV), for Two, Three, and Four Admolecules Adsorbed via the 1−2d and 1−2v Exoadditions along the Same Line on a (6,6) SWNT

	$2H_2$		$3H_2$		$4H_2$	
	E_a	μ	E_a	μ	E_a	μ
1−2d	−0.222	−0.664	−0.437	−0.867	−0.670	−1.371
1−2v	0.577	0.618	−0.368	−2.256	−1.962[a]	−6.745[a]

[a] Scission of the C—C bonds along the line causes unzipping of the tube and formation of a graphene sheet with hydrogenated edges, for which the current supercell is not appropriate. The actual binding strength is therefore greater than indicated in the table.

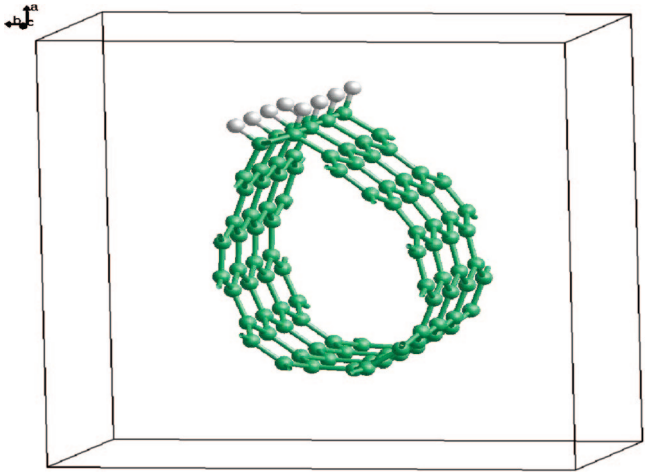

Figure 3. (6,6) SWNT with a row of 1−2d chemisorbed hydrogen.

chemical potential implies that the H_2 addition is energetically favored.

Starting from the singly hydrogenated CNT, the addition of another H_2 molecule is possible on all of the unoccupied sites of the H_2/SWNT complex. However, the sites that are well separated from the already occupied 1−2d site are unaffected by the already partially hydrogenated character of the CNT, and thus, the chemisorption at these locations remains endothermic. Hence, it is natural to explore the sites adjacent to the first two hydrogen atoms in the quest for favorable chemisorption in that they will be strongly perturbed relative to the rest of the CNT. Indeed, we find that these sites in close proximity to the existing hydrogens are more reactive toward chemisorption and the adjacent 1−2d site in the direction of the tube axis is the most exothermic of the sites investigated. A similar scenario applies for the third and the fourth admolecules; that is, once the first 1−2d exoaddition has taken place, the reaction keeps propagating parallel to the tube axis. Adsorption energies and chemical potentials for the additional three molecules are given in Table 2. In contrast to the energies for the first admolecule from Table 1, the values are negative. The nature of adsorption has changed from endothermic to exothermic with the addition of only one extra molecule. The two sets of values clearly indicate the trend of more exothermic chemisorption with increasing coverage. An average adsorption energy of −0.670 eV per molecule shows substantial improvement from 0.220 eV for the first admolecule. When the fourth molecule is added in the cell, a complete row of dissociated hydrogen has been created along the tube wall, as shown in Figure 3. Because of the formation of a complete row of sp^3-hybridized carbon atoms, this narrows the angle at this point of the nanotube, thereby allowing the opposite side to achieve lower curvature. It is this release of strain that provides the mechanism for the increasingly exothermic chemisorption trend.

TABLE 3: Adsorption Energies, E_a (eV), for Two, Three, Four, and Five Admolecules Adsorbed via the 1−2d and 1−2v Exoadditions along the Same Line on a Finite (6,6) SWNT

	H_2	$2H_2$	$3H_2$	$4H_2$	$5H_2$
1−2d	−0.204	−0.319	−0.471	−0.528	−0.564
1−2v	−1.119	−0.416	−0.676	−0.688	−1.995

TABLE 4: Adsorption Energies, E_a (eV), and Chemical Potentials, μ (eV), for a Single Admolecule on a (6,6) SWNT Predecorated with a Row of 1−2d Adsorbed Hydrogen[a]

	E_a (eV)	μ (eV)
$4H_2 + H_2^a$	−0.414	0.610
$4H_2 + H_2^{o\pm4}$	−0.387	0.746
$4H_2 + H_2^{o\pm3}$	−0.428	0.540
$4H_2 + H_2^{o\pm2}$	−0.492	0.220
$4H_2 + H_2^{o\pm1}$	−0.552	−0.077
$4H_2 + H_2^{o}$	−0.581	−0.221

[a] Attachment on the adjacent (a) and opposite (o) rows and any row in between ($o \pm i$, $i = 1-4$) was considered.

The results for 1−2v exoaddition in Table 2 indicate that, when the fourth H_2 is adsorbed (i.e., a full row), the nanotube opens up as a result of C—C bond cleavage. This effect has been previously reported[27] for small-diamater armchair SWNTs. As a result, a graphene sheet with hydrogenated ends is created. Although the graphene hydrogen storage capacity is worth investigating,[41] this subject is not pursued further in the present study. In fact, it will be shown below that, even for a (6,6) SWNT, the energetic barriers to the 1−2v pattern of addition make tube unzipping very unlikely to occur.

To investigate the difference between hydrogen adsorption on the finite and infinite models of the SWNT, the 1−2d and 1−2v exoadditions of H_2 at low coverage were also considered on the finite (6,6) nanotube. The first molecule was attached at the end of the SWNT, and subsequent admolecules were adsorbed along the same line until the whole row was hydrogenated. The calculated adsorption energies are given in Table 3. They are quite comparable to their counterparts on the infinite tube from Tables 1 and 2, except for the binding of the first molecule, which is already exothermic on the finite SWNT. This effect arises simply because the ends of the finite tube are the most reactive sites, which is also reflected in the larger binding strength for the 1−2v than for the 1−2d mechanism. Although the qualitative behavior of the finite and infinite nanotubes is the same with respect to hydrogen chemisorption, the fact that the end of the tube is the most reactive site of all influences the behavior. If hydrogen chemisorption occurs, then from a thermodynamic perspective, it is likely to begin at the ends of carbon nanotubes and then propagate along the tube from there.

The further hydrogenation of the periodic $4H_2$/SWNT system was also investigated by adsorbing another admolecule at one of six possible 1−2d sites, from a site adjacent (a) to the hydrogenated stripe to a site on the opposite side of the tube (o), as well as four intermediate sites ($o \pm i$, $i = 1-4$). The results are shown in Table 4. The results suggest that only additions in the vicinity of the opposite site are energetically favorable, that is, at the sites o and $o \pm 1$. The energy minimum is at a site on the opposite (o) side of the tube, as could be anticipated from the strain in the C—C bonds. If, instead of a single admolecule, two admolecules are adsorbed on a pair of

TABLE 5: Adsorption Energies, E_a (eV), and Chemical Potentials, μ (eV), for Two Admolecules 1−2d Attached along the Same Row of a (6,6) SWNT Predecorated with a Row of 1−2d Adsorbed Hydrogen[a]

	E_a (eV)	μ (eV)
$4H_2 + 2H_2^a$	−0.337	0.053
$4H_2 + 2H_2^{o\pm4}$	−0.319	0.029
$4H_2 + 2H_2^{o\pm3}$	−0.401	−0.262
$4H_2 + 2H_2^{o\pm2}$	−0.522	−0.668
$4H_2 + 2H_2^{o\pm1}$	−0.636	−1.056
$4H_2 + 2H_2^{o}$	−0.687	−1.222

[a] Attachment on the adjacent (a) and opposite (o) rows and any row in between (o ± i, i = 1−4) was considered.

TABLE 6: Adsorption Energies, E_a (eV), and Chemical Potentials, $\mu_{l,k}$ (eV), for a (6,6) SWNT Hydrogenated with l = 2, 3, 4, and 6 Stripes of H_2 via the 1−2d Exoaddition, As Illustrated in Figures 3 and 4

	E_a (eV)	μ (eV)
$2 \times 4H_2$	−0.905	−1.139
$3 \times 4H_2$	−0.761	−0.806
$4 \times 4H_2$	−0.633	−0.361
$6 \times 4H_2$	−0.361	0.040

neighboring 1−2d sites along the direction of the tube axis, the energies are similarly positioned relative to the distance from the hydrogenated row, as shown in Table 5. However, the DFT results indicate a favorable adsorption on a wider region of the tube, that is, from the opposite site to o ± 3. Again, the trend of increasingly favorable adsorption with the addition of one extra admolecule is manifest. The average adsorption energy is enhanced to −0.687 eV per molecule if the two admolecules are attached on opposite sides.

Rather than continuing the addition of individual molecules, from here onward, we consider the energetics of chemisorption when whole rows (i.e., four H_2 molecules per supercell) of hydrogen are attached at the favorable 1−2d sites along a (6,6) tube. Accordingly, we defined a modified chemical potential as the change in energy when $l - k$ extra rows of H_2 adsorb on a tube predecorated with k rows, so that there is a total of l stripes of H_2

$$\mu_{l,k} = [E^{tot}_{l\times 4H_2+NT} - E^{tot}_{k\times 4H_2+NT} - (l-k)4E^{tot}_{H_2}]/4(l-k) \quad (4)$$

Here, $E^{tot}_{k(l)\times 4H_2+NT}$ is the total energy of the CNT hydrogenated with k (l) rows of H_2. The denominator $4(l - k)$ ensures that the value of $\mu_{l,k}$ is given per admolecule, as per the associated adsorption energy. A (6,6) tube was decorated with two, three, four, and six stripes of hydrogen, in a symmetric fashion, so as to maximize the distance between the hydrogens. The optimized geometries are shown in Figure 4, and the corresponding energies are given in Table 6. An adsorption energy of −0.905 eV, with the corresponding chemical potential of −1.139 eV, for the tube with two hydrogen stripes opposite to each other is the energy minimum.[46] The associated chemical potentials are still negative for the tubes with three and four hydrogen stripes, which implies that the 1−2d exoaddition of up to four rows (i.e., a coverage of $^1/_3$ ML) of hydrogen is energetically favorable. However, the addition of three extra stripes to the tube with three existing rows (a total of six rows or, equivalently, a coverage of $^1/_2$ ML) might not be favorable, at least not for all of the extra admolecules. The chemical potential for such a process becomes slightly positive, and even though the average adsorption energy is still negative, the direction of the reaction has been reversed. This result demonstrates that, in equilibrium at very low pressure, a (6,6) SWNT is potentially capable of exothermically adsorbing between $^1/_3$ and $^1/_2$ ML of hydrogen via the 1−2d exoaddition.

While further hydrogen addition does not appear possible under equilibrium conditions, this does not imply that more hydrogen cannot be stored in nanotubes under different conditions, such as under a high hydrogen pressure or through the use of an incident hydrogen beam. The stabilities of the tubes hydrogenated in such ways are determined by the respective binding energies. We have inspected four structures that correspond to fully hydrogenated nanotubes with high azimuthal symmetry. Their optimized geometries are shown in Figure 5, and calculated adsorption energies are given in Table 7.

The structure in Figure 5a is achieved by endohydrogenation of unsaturated carbon atoms from the last structure in Figure 4. As per the outer face, the attachment of H_2 on the inner face follows the 1−2d pattern. An adsorption energy of −0.286 eV per molecule for this configuration indicates a further reduction in binding strength from the structures with three and six H stripes in Figure 4. Nevertheless, such an energy suggests that the structure, if it can be formed, is probably stable at room temperature.

The configuration in Figure 5b is formed by either 1−2v or 1−4 exo- and endohydrogenation. The evaluated adsorption energy of −0.173 eV implies a rather low degree of stability and the structure could easily undergo a transformation in which most hydrogen would be desorbed, whereas the rest could recombine with C atoms to make a more stable hydrocarbon complex, possibly a graphene sheet with hydrogenated ends.

The structure in Figure 5c is the most interesting because, with an adsorption energy of −0.618 eV per molecule, it promises great stability. The unusual binding strength of this structure, termed "zigzag" [29] and "uniform",[26] has been noted in previous computational studies.[28–31] The geometry can be viewed as being formed via the 1−3 mode of exo- and endohydrogenation. However, there are problems with this

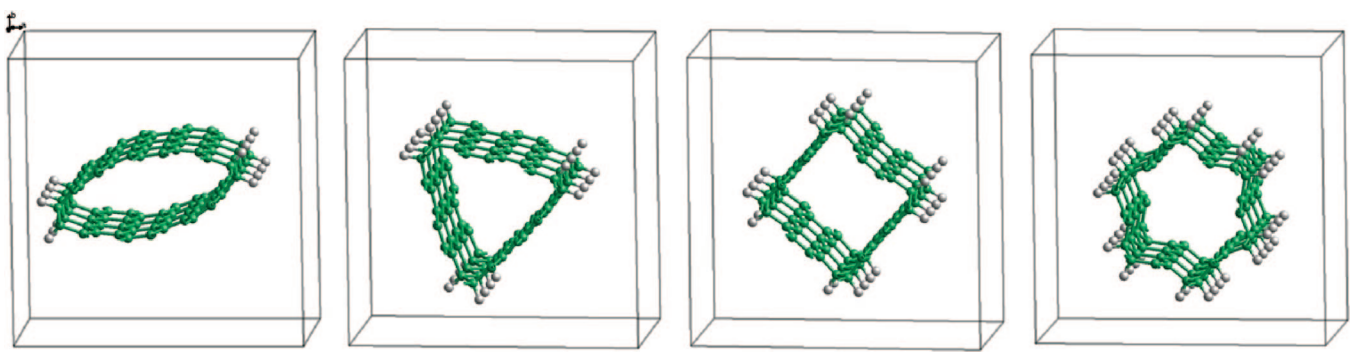

Figure 4. (6,6) SWNT with two, three, four, and six stripes of 1−2d chemisorbed hydrogen.

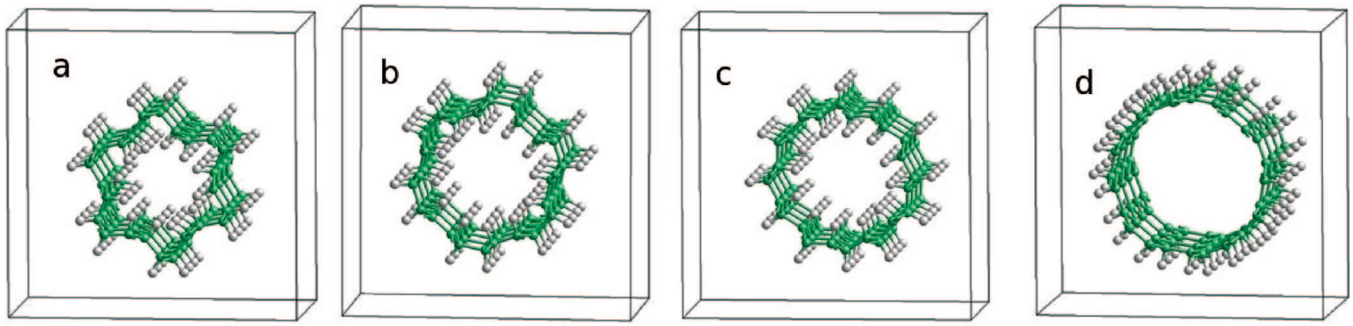

Figure 5. Optimized structures of fully hydrogenated (6,6) SWNT. (a) Generated by the 1−2d addition of H_2 molecules on the outer and inner faces. (b) Formed by either the 1−2v or 1−4 addition of H_2 molecules on the outer and inner faces. (c) Created by the 1−3 addition of H_2 molecules on the outer and inner faces. (d) Exohydrogenation at 1 ML.

TABLE 7: Adsorption Energies, E_a (eV), for the Fully Hydrogenated Structures Shown in Figure 5

structure	E_a (eV)
a	−0.286
b	−0.173
c	−0.618
d	0.965

TABLE 8: Adsorption Energies, E_a (eV), for a (6,6) SWNT Decorated with One to Six Stripes of Hydrogen via the 1−3 Exoaddition

	E_a (eV)
$4H_2$	1.741
$2 \times 4H_2$	1.347
$3 \times 4H_2$	1.844
$4 \times 4H_2$	2.194
$6 \times 4H_2$	N/A

TABLE 9: Adsorption Energies, E_a (eV), for a (6,6) SWNT Hydrogenated with One, Two, Four, and Six Rows of Hydrogen via the Combined Exo/Endo 1−2d Attachment

	E_a (eV)
$4H_2$	0.261
$2 \times 4H_2$	−0.180
$4 \times 4H_2$	−0.199
$6 \times 4H_2$	−0.262

mechanism. First, as Table 1 shows, this pattern of attachment is the least favorable at low coverage. Second, the energetics of 1−3 exohydrogenation, unlike that of the 1−2d addition, does not exhibit any improvement with the coverage. On the contrary, as Table 8 demonstrates, the evaluated adsorption energies for the SWNT with one, two, three, four, and six rows of 1−3 attached hydrogen become increasingly endothermic with coverage. In fact, the configuration with six stripes is not even metastable, but spontaneously rearranges toward the analogous structure of the 1−2d exoaddition (the right panel in Figure 4), as demonstrated by Gülseren et al.[26] and reproduced in the present work. Alternatively, the fully saturated structure in Figure 5c can be obtained again by a 1−2d pattern of attachment, in which one C atom is exohydrogenated and its counterpart endohydrogenated. The adsorption energies, given in Table 9, show that this is a far more favorable process. The trend of gradually increasing binding strengths is evident, and at $^1/_2$ ML (i.e., six rows of H_2), it reaches about 50% of the value at 1 ML.

Finally, a fully exohydrogenated (6,6) nanotube, shown in Figure 5d, with an adsorption energy of 0.965 eV, is very unfavorable, even if metastable. The reason for this lies with the constraints of geometry and symmetry, which prevent the C atoms from forming four sp^3 bonds with angles that are close to tetrahedral.[29] The bonds are thus more strained than those in structures a−c.

TABLE 10: Activation Energies (eV), for the Exoadditions of the First, Second, And the Fourth (Full Row) of H_2 Molecules along a Line of a (6,6) SWNT, via the 1−2d and 1−2v Mechanisms

	first	second	fourth
1−2d	3.46	2.85	1.87
1−2v	3.58	2.53	2.59

The full monolayer limit corresponds to gravimetric $^1/_{13}$ or 7.7 wt % hydrogen uptake. Therefore, the present results clearly demonstrate that CNTs have the potential to achieve a viable hydrogen storage density via the mechanism of chemisorption. However, the fact that highly protonated CNTs are not experimentally observed reflects the activated nature of the process. For the chemisorption of a single admolecule on a (6,6) SWNT, an activation energy of ca. 2−2.5 eV has been reported.[6,24] Therefore, the onset of chemisorption is not only endothermic, but also highly improbable at room temperature. We evaluated kinetic barriers for the exoaddition of the first, second, and fourth (i.e., a full row) H_2 molecule adsorbed along a row via both the 1−2d and 1−2v mechanisms. The results for these processes are shown in Table 10. For the first admolecule, both mechanisms result in large barriers of ∼3.5 eV, which substantially exceed those previously reported. This most likely occurs because of differences in the computational techniques. In the previous work,[6,24] a simple "drag" method was used to identify the transition states; that is, the molecule ws pushed stepwise closer to the axis of the tube. The well-known shortcoming of the method is that it causes slipping from the minimum-energy path (MEP), and the true transition state is therefore not found. This fact is made manifest by the energy vs distance curves, which exhibit a spike at the point taken as the transition state and then a sudden drop beyond that point. In contrast, we freeze the distance between the two C−H pairs of atoms using internal coordinates, while relaxing all other degrees of freedom. This was achieved using the geometry based on a hybrid Z-matrix Cartesian scheme.[42] The result is an MEP with a harmonic potential around the maximum, taken as the transition state. The present findings demonstrate that the onset of hydrogenation is even more difficult than previously estimated. However, the values for the second molecule of ∼2.5 eV, attached either by the 1−2d or 1−2v mechanism, indicate that the kinetics of chemisorption improves with the coverage as well. However, this trend continues only for the 1−2d addition for which the fourth molecule experiences a barrier of only 1.87 eV, whereas in the case of the 1−2v addition, no further drop in barrier is found, as shown in Table 10.

It has been reported before that the 1−2v exoaddition of a full row of hydrogen can cause the scission of the C—C bonds along the SWNT and the formation of graphene sheet with hydrogen-terminated edges.[6,27] We investigated both the energetics and kinetics of this process, with the relevant results shown in Tables 2 (3 for the finite tube) and 10, respectively. Unlike for the 1−2d mechanism, the addition of the second molecule does not show any improvement in the adsorption energy. However, the situation changes dramatically for the third and fourth admolecules, when the scission of C—C bonds becomes manifest and the binding strengths sharply increase. In the case of the fourth admolecule, the tube completely opens up, and the supercell is not appropriate to accommodate such a geometry, so the corresponding values in Table 2 are not final, but are expected are to drop further to a more negative magnitude. The corresponding values for the finite nanotube in Table 3 are valid though. However, the kinetics of the process, as indicated above, does not follow the trend because the barriers in Table 10 do not decrease. Hence, even though the 1−2v exoaddition of a full row of hydrogen is more beneficial energetically, it is less likely to occur than the corresponding 1−2d addition.

In general, the barriers evaluated in the present work are quite high for adsorption, and the rates of possible annealing processes can remain very low, indicating the difficulty of reaching thermal equilibrium. The structure of the tube would then result from kinetic, rather than thermodynamic, control of the reaction. Because CNTs are typically produced with somewhat larger diameters, ca. 12−14 Å,[43,44] which correspond to armchair (9,9) and (10,10) SWNTs, both the thermodynamics and kinetics of hydrogen chemisorption are expected to be less favorable than on the (6,6) tube investigated in the current work. As Figure 2 of ref 24 illustrates, for tubes of very small diameter, such as (3,3) and (4,4), the calculated activation barrier for H_2 chemisorption is less than 0.3 eV and leads to potential wells of ca. −2 and −0.25 eV, respectively. In contrast, for a graphene sheet, only a potential energy wall is encountered as the molecule approaches (the GGA does not predict a physisorbed potential energy well). Larger CNTs have smaller curvature and, therefore, with respect to hydrogen chemisorption, behave much like a graphene sheet. In fact, the results of Yildirim et al.[25] demonstrate that an SWNT with a radius larger than ca. 6.25 Å, which corresponds to an (8,8) armchair or (12,0) zigzag tube, is thermodynamically driven to be partially, rather than fully, hydrogenated. Therefore, on the basis of the results of the present work and related studies, it seems that only subnanometer carbon tubes, with diameters up to 10 Å, have the theoretical potential for a high hydrogen uptake via the mechanism of chemisorption. On the other hand, the usefulness of hydrogen storage in this way is questionable given that the extraction of hydrogen, although feasible,[21,22] would be quite impractical.

IV. Conclusions

We have modeled the energetics of hydrogen chemisorption on a (6,6) nanotube using gradient-corrected density functional theory. The adsorption was investigated over a range of coverages, from close to the zero limit to a full monolayer. We found that the attachment of the first isolated admolecule on the tube is endothermic. However, with increasing coverage, the character of chemisorption dramatically changes to exothermic, making the dissociative addition of new H_2 molecules increasingly favorable. We explored possible routes for the formation of energetically favorable fully hydrogenated nanotubes. The mechanism termed the 1−2d exoaddition is predicted to have the potential of adsorbing between $^1/_3$ and $^1/_2$ ML of hydrogen on the outer face of the tube. The initial kinetics of such a process is predicted to proceed at an increasing rate with increasing degree of coverage. If a modified mechanism is considered, a combined 1−2d exo-/endoaddition, full saturation of the tube is predicted, resulting in an adsorption energy of −0.618 eV per molecule and a hydrogen uptake of 7.7 wt %. The fact that such structures are not observed experimentally is attributed to the highly activated nature of the dissociative chemisorption and the less reactive character of larger, more realistic nanotubes.

Acknowledgment. We thank the Australian Research Council for financial support through a Discovery grant. The use of supercomputer facilities at the Australian Partnership for Advanced Computing (APAC) and iVEC is gratefully acknowledged. J.D.G. thanks the Government of Western Australia for support through a Premier's Research Fellowship.

References and Notes

(1) Hynek, S.; Fuller, W.; Bentley, J. *Int. J. Hydrogen Energy* **1997**, *22*, 601.
(2) Dillon, A. C.; Jones, K. M.; Bekkedahl, T. A.; Kiang, C. H.; Bethune, D. S.; Heben, M. J. *Nature* **1997**, *386*, 377.
(3) Liu, C.; Fan, Y. Y.; Liu, M.; Cong, H. T.; Cheng, H. M.; Dresselhaus, M. S. *Science* **1999**, *286*, 1127.
(4) Stan, G.; Cole, M. W. *J. Low Temp. Phys.* **1998**, *110*, 539.
(5) Arellano, J. S.; Molina, L. M.; Rubio, A.; Alonso, J. A. *J. Chem. Phys.* **2000**, *112*, 8114.
(6) Arellano, J. S.; Molina, L. M.; Rubio, A.; Lopez, M. J.; Alonso, J. A. *J. Chem. Phys.* **2002**, *117*, 2281.
(7) Cheng, H.; Pez, G. P.; Cooper, A. C. *J. Am. Chem. Soc.* **2001**, *123*, 5845.
(8) Volpe, M.; Cleri, F. *Chem. Phys. Lett.* **2003**, *371*, 476.
(9) Xia, Y. Y.; Zhu, J. Z. H.; Zhao, M. W.; Li, F.; Huang, B. D.; Ji, Y. J.; Liu, X. D.; Tan, Z. Y.; Song, C.; Yin, Y. Y. *Phys. Rev. B* **2005**, *71*, 075412.
(10) Lu, A. J.; Pan, B. C. *Phys. Rev. B* **2005**, *71*, 165416.
(11) Nutznadel, C.; Züttel, A.; Chartouni, D.; Schlapbach, L. *Electrochem. Solid-State Lett.* **1999**, *2*, 30.
(12) Lee, S. M.; Park, K. S.; Choi, Y. C.; Park, Y. S.; Bok, J. M.; Bae, D. J.; Nahm, K. S.; Choi, Y. G.; Yu, S. C.; Kim, N.; Frauenheim, T.; Lee, Y. H. *Synth. Met.* **2000**, *113*, 209.
(13) Ye, Y.; Ahn, C. C.; Witham, C.; Fultz, B.; Liu, J.; Rinzler, A. G.; Colbert, D.; Smith, K. A.; Smalley, R. E. *Appl. Phys. Lett.* **1999**, *74*, 2307.
(14) Kolesnikov, A. I.; Bashkin, I. O.; Antonov, V. E.; Colognesi, D.; Mayers, J.; Moravskye, A. P. *J. Alloys Compd.* **2007**, *446*, 389.
(15) Khare, B. N.; Meyyappan, M.; Kralj, J.; Wilhite, P.; Sisay, M.; Imanaka, H.; Koehne, J., Jr *Appl. Phys. Lett.* **2002**, *81*, 5237.
(16) Zhang, G. Y.; Qi, P. F.; Wang, X. R.; Lu, Y. R.; Mann, D.; Li, X. L.; Dai, H. J. *J. Am. Chem. Soc.* **2006**, *128*, 6026.
(17) Buchs, G.; Krasheninnikov, A. V.; Ruffieux, P.; Groning, P.; Foster, A. S.; Nieminen, R. M.; Groning, O. *New J. Phys.* **2007**, *9*, 275.
(18) Zhang, G.; Li, Q.; Jiang, K.; Zhang, X.; Chen, J.; Ren, Z.; Fan, S. *Nano Lett.* **2007**, *7*, 1622.
(19) Miller, G. P.; Kintigh, J.; Kim, E.; Weck, P. W.; Berber, S.; Tománek, D.; Fan, S. *J. Am. Chem. Soc.* **2008**, *130*, 2296.
(20) Ma, Y. C.; Xia, Y. Y.; Zhao, M. W.; Wang, R. J.; Mei, L. M. *Phys. Rev. B* **2001**, *63*, 115422.
(21) Nikitin, A.; Ogasawara, H.; Mann, D.; Denecke, R.; Zhang, Z.; Dai, H.; Cho, K.; Nilsson, A. *Phys. Rev. Lett.* **2005**, *95*, 225507.
(22) Nikitin, A.; Li, X.; Zhang, Z.; Ogasawara, H.; Dai, H.; Nilsson, A. *Nano Lett.* **2008**, *8*, 162.
(23) Chan, S. P.; Chen, G.; Gong, X. G.; Liu, Z. F. *Phys. Rev. Lett.* **2001**, *87*, 205502.
(24) Tada, K.; Furuya, S.; Watanabe, K. *Phys. Rev. B* **2001**, *6315*, 155405.
(25) Yildirim, T.; Gülseren, O.; Ciraci, S. *Phys. Rev. B* **2001**, *64*, 075404.
(26) Gülseren, O.; Yildirim, T.; Ciraci, S. *Phys. Rev. B* **2002**, *66*, 121401.
(27) Lu, G.; Scudder, H.; Kioussis, N. *Phys. Rev. B* **2003**, *68*, 205416.
(28) Lee, S. M.; Lee, Y. H. *Appl. Phys. Lett.* **2000**, *76*, 2877.
(29) Lee, S. M.; An, K. H.; Lee, Y. H.; Seifert, G.; Frauenheim, T. *J. Am. Chem. Soc.* **2001**, *123*, 5059.
(30) Lee, S. M.; An, K. H.; Kim, W. S.; Lee, Y. H.; Park, Y. S.; Seifert, G.; Frauenheim, T. *Synth. Met.* **2001**, *121*, 1189.
(31) Seifert, G. *Solid State Ionics* **2004**, *168*, 265.

(32) Sánchez-Portal, D.; Ordejón, P.; Artacho, E.; Soler, J. M. *Int. J. Quantum Chem.* **1997**, *65*, 453.

(33) Soler, J. M.; Artacho, E.; Gale, J. D.; García, A.; Junquera, J.; Ordejón, P.; Sánchez-Portal, D. *J. Phys.: Condens. Matter* **2002**, *14*, 2745.

(34) Kleinman, L.; Bylander, D. M. *Phys. Rev. Lett.* **1982**, *48*, 1425.

(35) Troullier, N.; Martins, J. L. *Phys. Rev. B* **1991**, *43*, 1993.

(36) Perdew, J. P.; Burke, K.; Ernzerhof, M. *Phys. Rev. Lett.* **1996**, *77*, 3865.

(37) Sankey, O. F.; Niklewski, D. J. *Phys. Rev. B* **1989**, *40*, 3979.

(38) Junquera, J.; Paz, Ó.; Sánchez-Portal, D.; Artacho, E. *Phys. Rev. B* **2001**, *64*, 235111.

(39) Dinadayalane, T. C.; Kaczmarek, A.; Lukaszewicz, J.; Leszczynski, J. *J. Phys. Chem. C* **2007**, *111*, 7376.

(40) Kaczmarek, A.; Dinadayalane, T. C.; Lukaszewicz, J.; Leszczynski, J. *Int. J. Quantum Chem.* **2007**, *107*, 2211.

(41) Roman, T.; Diño, W. A.; Nakanishi, H.; Kasai, H.; Sugimoto, T.; Tange, K. *Jpn. J. Appl. Phys.* **2006**, *45*, 1765.

(42) Hoft, R. C.; Gale, J. D.; Ford, M. J. *Mol. Sim.* **2006**, *32*, 593.

(43) Dresselhaus, M. S.; Dresselhaus, G.; Eklund, P. C. *Science of Fullerenes and Carbon Nanotubes*; Academic Press: New York, 1996.

(44) Vigolo, B.; Pénicaud, A.; Coulon, C.; Sauder, C.; Pailler, R.; Journet, C.; Bernier, P.; Poulin, P. *Science* **2000**, *290*, 1331.

(45) The average energy E_b per C—H bond (i.e., H atom) can be evaluated as $E_b = {}^1/_2(E_a + E_{dissoc})$, where E_a is the average adsorption energy per hydrogen molecule and the H_2 dissociation energy, $E_{dissoc} = E^{tot}_{H_2} - 2E^{tot}_{H}$, is evaluated here to be −4.32 eV.

(46) The structure with two hydrogen stripes exhibits the most elongated profile of the tube, and it was used to test the effects of the supercell size on the accuracy of the computed energetics. First, the tube was rotated about its axis so that the two symmetry planes were parallel with the cell size, thus maximizing the overlap with the images in two adjacent supercells. An energy of −0.902 eV was obtained in this orientation. Then, the cell size was extended to 28 Å so that the overlap vanished. In this larger cell, the corresponding energy was −0.899, which verifies that the smaller supercell gives satisfactory accuracy.

JP802104N